SUPPLEMENTAL DATA

Molecular dynamics simulations of forced unbending of integrin $\alpha_V\beta_3$

Wei Chen, Jizhong Lou, Jen Hsin, Klaus Schulten, Stephen C. Harvey, and Cheng Zhu

Supplemental Methods

Building complete ectodomain models of unliganded and liganded integrin $\alpha_V\beta_3$

The first crystal structure of unliganded integrin $\alpha_V\beta_3$ ectodomain (PDB code 1U8C (Xiong et al., 2004)) did not resolve the α_V EE' loop (residue 839-867), the β_3 PSI-hybrid linker (residue 51-53), and the β_3 EGF1 and EGF2 domains (residue 435-522). The EE' loop contains the proteolytic site after Arg860 that generates the heavy and light chains in matured α_V (Suzuki et al., 1987). Because this loop is flexible and does not interact with other domains, we left it out in our simulations. To add the missing EGF1 and EGF2 domains, we used the crystal structure of a β_2 fragment (PDB code 2P28 (Shi et al., 2007)) as a template because β_2 and β_3 have ~41% sequence identity and ~54% similarity in the region containing the PSI, EGF1, and EGF2 domains (Fig. S1A). The hybrid and EGF3 domains in the 1U8C structure was first aligned to the corresponding domains in the 2P28 structure (Fig. S1B). MODELLER (Sali and Blundell, 1993) was used to build the PSI, EGF1, and EGF2 domains with the hybrid and EGF3 domains fixed. PSI was taken into account to avoid clashes between PSI and EGF1 and assure a long-distance disulfide bond between PSI and EGF1 (Cys13-Cys435). The β_3 fragment model so obtained includes the PSI, hybrid, EGF1, EGF2, and EGF3 domains, which had similar quality as the β_2 template according to the discrete optimized protein energy (DOPE) (Fig. S1F).

Because the β_2 template is in an extended conformation, our initial β_3 model was also extended. To fit this β_3 model into the bent $\alpha_V\beta_3$ structure, we performed a TMD simulation

without solvation using AMBER8 (Case et al., 2004). The extended model was first equilibrated for 1 ns (Fig. S1E). The hybrid domain in the β_3 model was then forced to move towards the hybrid domain of the bent $\alpha_V\beta_3$ with a force constant of 0.01 kcal mol^{-1} $Å^{-2}$ with the EGF3 domain constrained. In the first ns of the bending simulation, the β_3 model gradually bent over (Fig. S1C) and the RMSD relative to the bent structure for all the heavy atoms of the PSI, hybrid, and EGF3 domains decreased from ~100 Å to ~9 Å. The PSI, hybrid, and EGF3 domains were next forced to move towards the corresponding domains in the bent $\alpha_V\beta_3$ with a force constant of 0.1 kcal mol^{-1} $Å^{-2}$. Finally, the force constant was increased to 1 kcal mol^{-1} $Å^{-2}$, yielding the final RMSD of ~1 Å. The bent β_3 model so obtained had no major conflicts with the α_V subunit in the 1U8C structure (Fig. S1D). The PSI-hybrid linker (residue 51-53) and the EGF1 and EGF2 domains (residue 435-522) from the bent β_3 model were added to the original 1U8C structure to generate a complete model of the unliganded integrin $\alpha_V\beta_3$ ectodomain (i.e. U1).

The crystal structure of integrin $\alpha_V\beta_3$ ectodomain liganded with a cyclic-RGD ligand (PDB code 1L5G (Xiong et al., 2002)) did not resolve the α_V EE' loop (residue 839-867), the β_3 PSI domain (residue 1-54), and the β_3 EGF1 and EGF2 domains (residue 435-531). Because the 1L5G structure is nearly identical to the 1U8C structure except for regions near the ligand-binding site at the βA domain, we simply added the PSI domain (residue 1-56) and the EGF1, EGF2, and part of EGF3 domains (residue 435-548) from the bent β_3 model to the 1L5G structure to obtain a complete model for the liganded integrin $\alpha_V\beta_3$ ectodomain (i.e. L1).

Supplemental Figure Legends

Figure S1. Building complete ectodomain models of integrin $\alpha_V\beta_3$. A. Amino acid sequence alignment between β_2 and β_3 in the region containing the PSI, EGF1, and EGF2 domains with ClustalW2 (Larkin et al., 2007). **B.** Alignment of the template and the homology model. On the left, the hybrid and EGF3 domains (blue) from the crystal structure of integrin $\alpha_V\beta_3$ (PDB code 1U8C) were aligned to the template (gray) of the β_2 fragment (PDB code 2P28) before homology modeling. On the right, the final homology model (red) was compared to the template. **C.** Targeting the extended β_3 model (red) to the bent β_3 structure (gray) by TMD simulation. Snapshots were taken at indicated times. **D.** The final bent β_3 model (red) in the bent $\alpha_V\beta_3$ structure (α_V, yellow; β_3, gray). **E.** RMSD relative to the bent structure for all heavy atoms of the PSI, hybrid, and EGF3 domains during the TMD simulation. **F.** Comparison of the DOPE score of the homology model with the template.

Figure S2. Comparison of the homology model of the EGF1 and EGF2 domains with the crystal structure. On the left and middle, structures were aligned on Cα atoms of other parts of β_3 than the EGF1 and EGF2 domain. On the right, the EGF1 and EGF2 domains were aligned on their own Cα atoms. The homology model is in red and the crystal structure (PDB code 3IJE) is in blue.

Figure S3. Changes in headpiece-tailpiece interactions interactions at the major force peaks. Buried SASAs (upper row, left ordinate) and numbers of H-bonds (lower row, left ordinate) of hybrid (blue), βA (cyan), EGF4 (red), and βTD (magenta) domains as well as pulling force (gray,

both rows, right ordinate) were plotted vs. simulation time for the U1 SMD 2 (left column) and U1 SMD 3 (right column). Some of the curves were obscured due to overlapping.

Figure S4. H-bonds at the hybrid/EGF4 interface of U2. The starting structures at the hybrid/EGF4 interface of U2 are shown. Residues involved in H-bonds are shown as sticks. H-bonds are indicated by dashed lines. The hybrid and EGF4 domains are colored in orange and tan, respectively.

Figure S5. Changes in headpiece-tailpiece interactions during the unbending of the liganded $\alpha_V\beta_3$. Buried SASAs (colored, left ordinate) of indicated domains were plotted vs. simulation time along with pulling force (gray, right ordinate) in L1 SMD 1 and L2 SMD.

Figure S6. Amino acid sequence alignment of the α_V subunit. The sequences were aligned across species (**A**) or human α family members (**B**) by using ClustalW2 (Larkin et al., 2007). The sequences were retrieved from UniProt Knowledgebase (UniProtKB) (Jain et al., 2009). Conserved mutations at residue 457 and the α-genu metal ion site are highlighted. "*" indicates identical residues, ":" indicates conserved substitutions, and "." indicates semi-conserved substitutions.

Supplemental Movie Legends

Movie S1. Unbending of unliganded integrin $\alpha_V\beta_3$ in U1 SMD 1. The COM of the Cα atoms of the central β sheet of the βA domain was pulled and the COM of the Cα atoms of the βTD

was constrained. The running simulation time is indicated. The α_V subunit was in cyan and the β_3 subunit was in pink. The same color coding was used in all movies.

Movie S2. Unbending of unliganded integrin $\alpha_V\beta_3$ in U2 SMD. The COM of the Cα atoms of the central β sheet of the βA domain was pulled and the COM of the Cα atoms of the βTD was constrained.

Movie S3. Rebending of partially-extended unliganded integrin $\alpha_V\beta_3$ in U1 free MD 1. The simulation started from the partially-extended structure that was selected from U1 SMD 1. Nothing was constrained during the simulation. The bent structure is in gray for comparison.

Movie S4. Relaxation of fully-extended unliganded integrin $\alpha_V\beta_3$ in U1 free MD 2. The simulation started from the fully-extended structure that was selected from U1 SMD 1. Nothing was constrained during the simulation.

Movie S5. Unbending of liganded integrin $\alpha_V\beta_3$ in L1 SMD 1. The COM of Cα atoms of the RGD ligand (green spheres) was pulled and the COM of the Cα atoms of the βTD was constrained.

Movie S6. Unbending of liganded integrin $\alpha_V\beta_3$ in L2 SMD. The COM of the Cα atoms of the RGD ligand (green spheres) was pulled and the COM of the Cα atoms of the βTD was constrained.

Supplemental Reference

Jain, E., Bairoch, A., Duvaud, S., Phan, I., Redaschi, N., Suzek, B.E., Martin, M.J., McGarvey, P., and Gasteiger, E. (2009). Infrastructure for the life sciences: design and implementation of the UniProt website. BMC Bioinformatics *10*, 136.

Larkin, M.A., Blackshields, G., Brown, N.P., Chenna, R., McGettigan, P.A., McWilliam, H., Valentin, F., Wallace, I.M., Wilm, A., Lopez, R., *et al.* (2007). Clustal W and Clustal X version 2.0. Bioinformatics *23*, 2947-2948.

Sali, A., and Blundell, T.L. (1993). Comparative protein modelling by satisfaction of spatial restraints. J Mol Biol *234*, 779-815.

Suzuki, S., Argraves, W.S., Arai, H., Languino, L.R., Pierschbacher, M.D., and Ruoslahti, E. (1987). Amino acid sequence of the vitronectin receptor alpha subunit and comparative expression of adhesion receptor mRNAs. J Biol Chem *262*, 14080-14085.

Supplemental Figure S1

Click here to download high resolution image

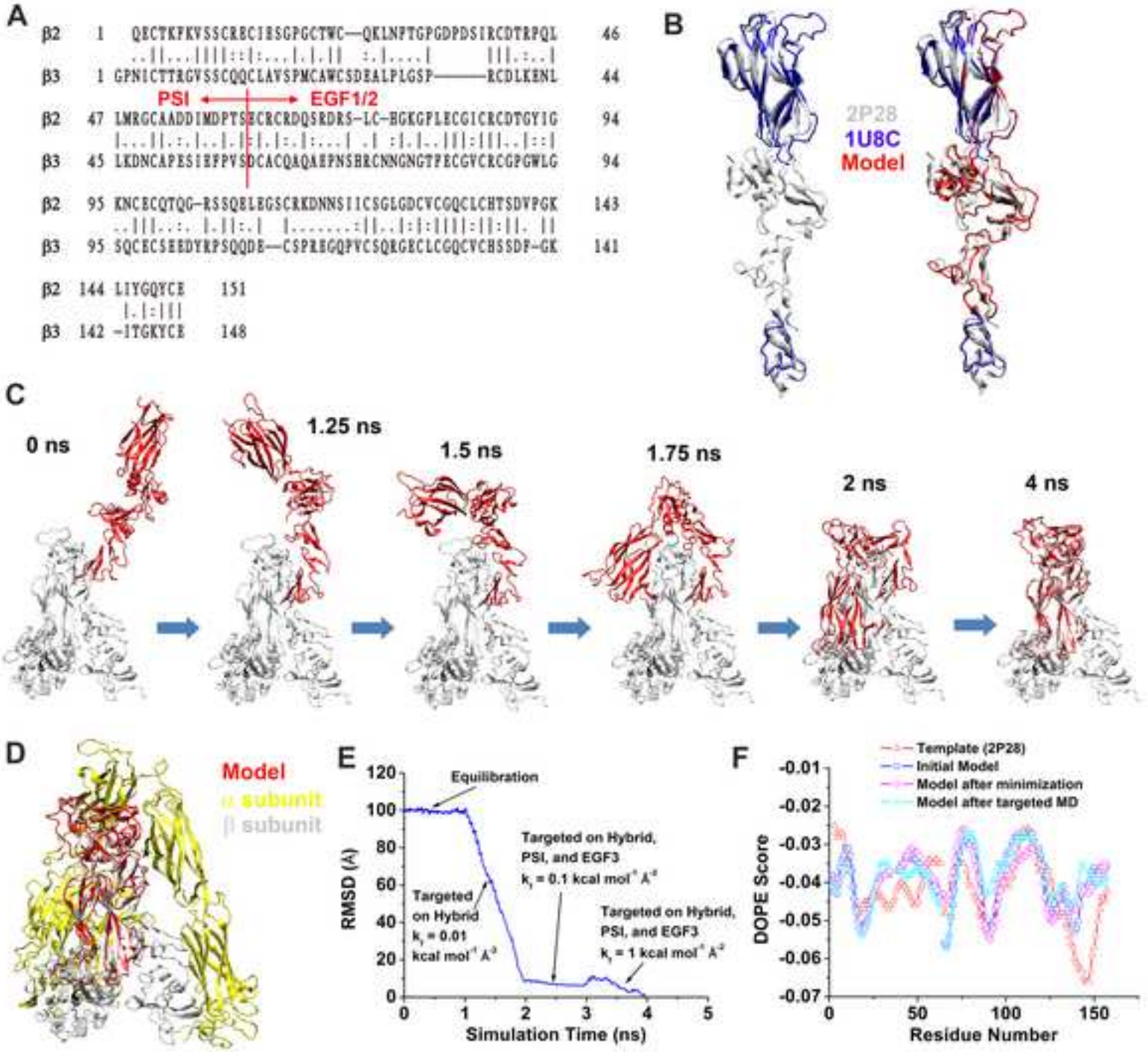

Supplemental Figure S2

Click here to download high resolution image

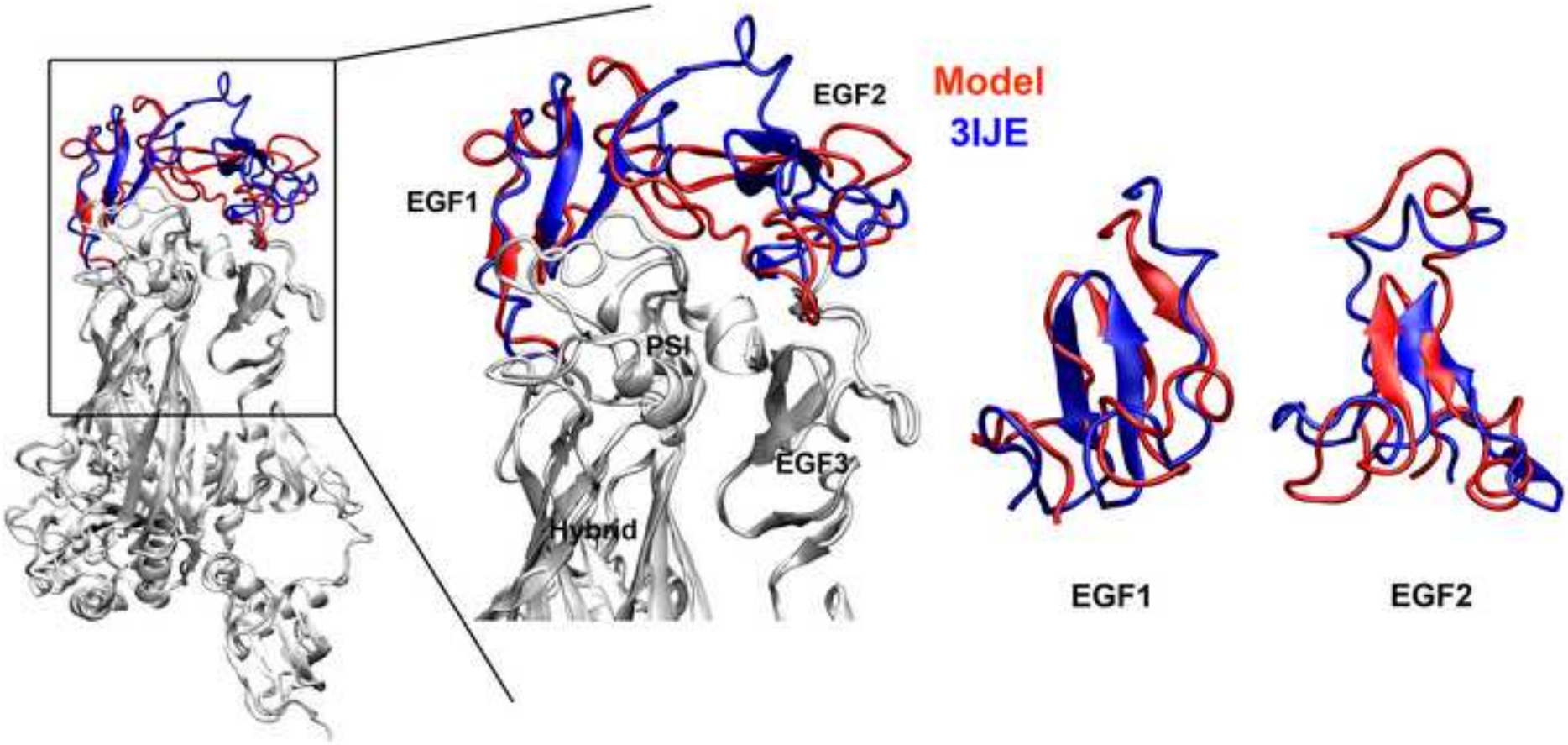

Supplemental Figure S3

Click here to download high resolution image

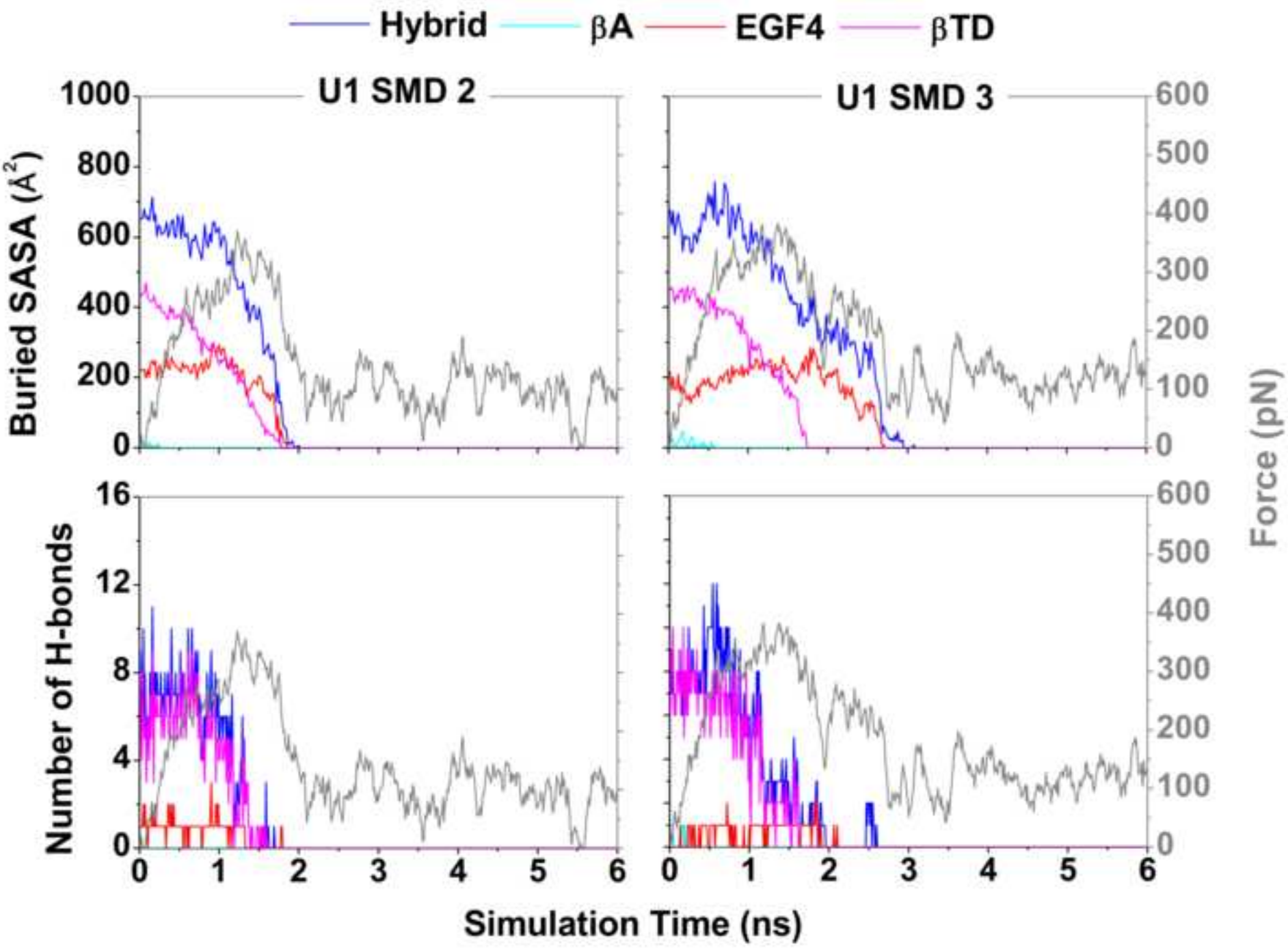

Supplemental Figure S4

Click here to download high resolution image

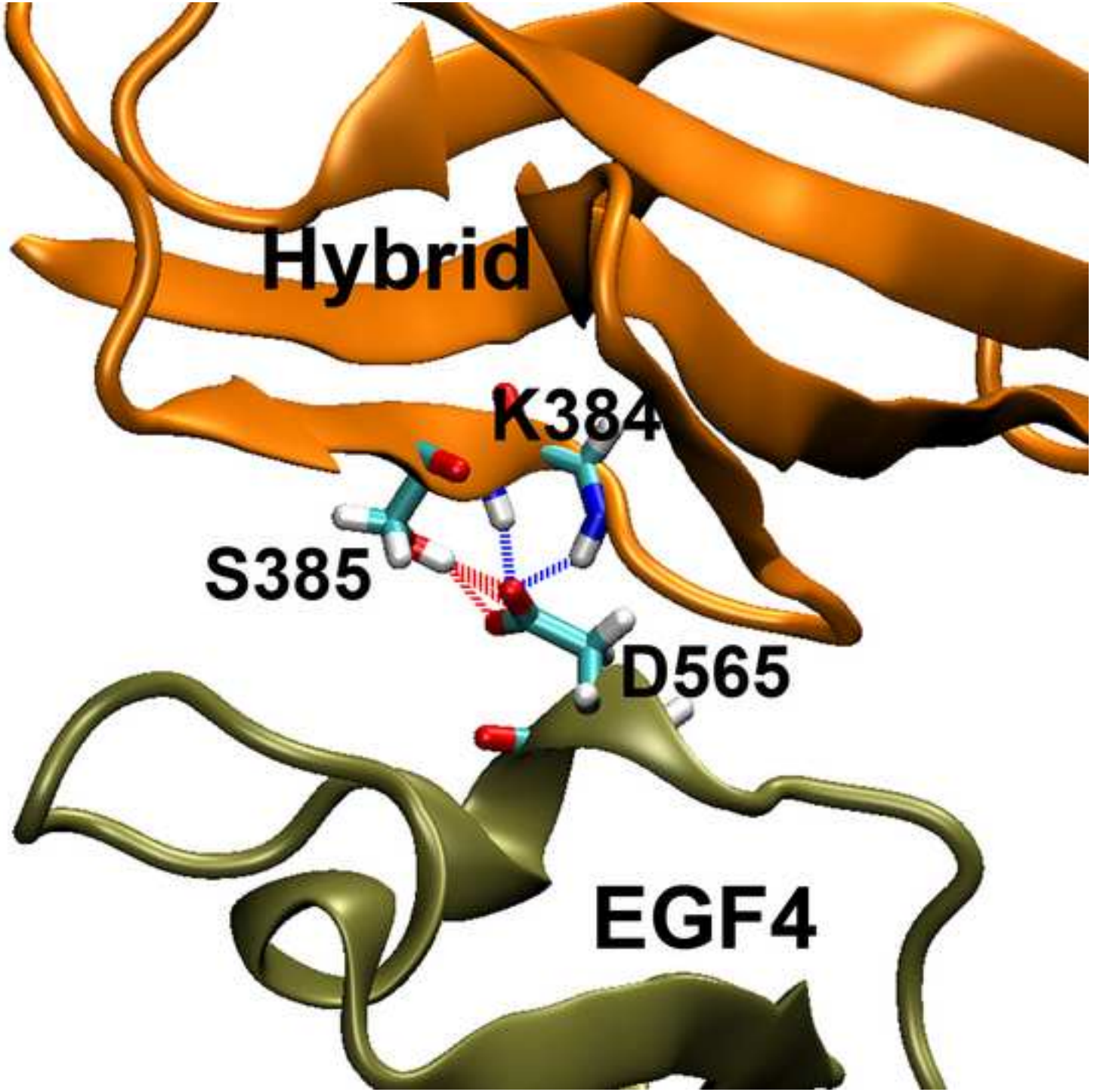

Supplemental Figure S5

Click here to download high resolution image

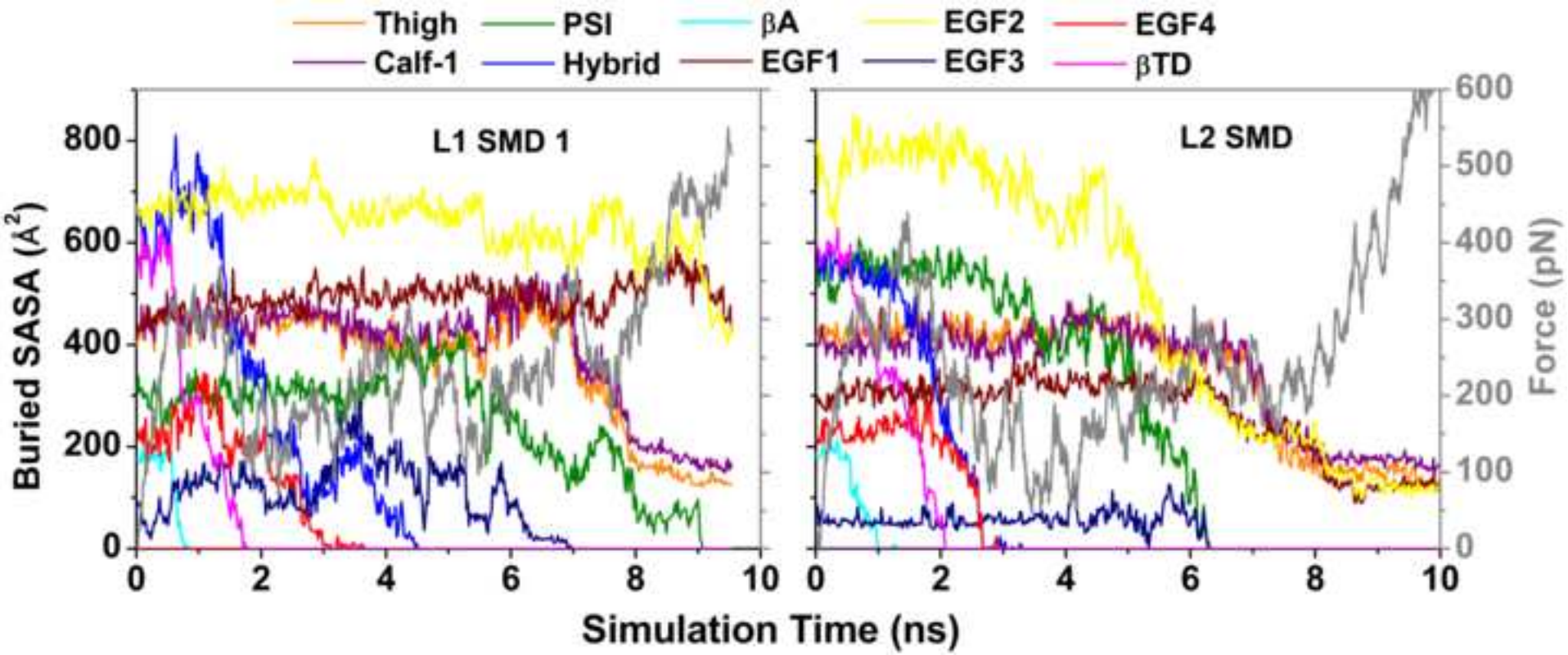

Supplemental Figure S6

Click here to download high resolution image

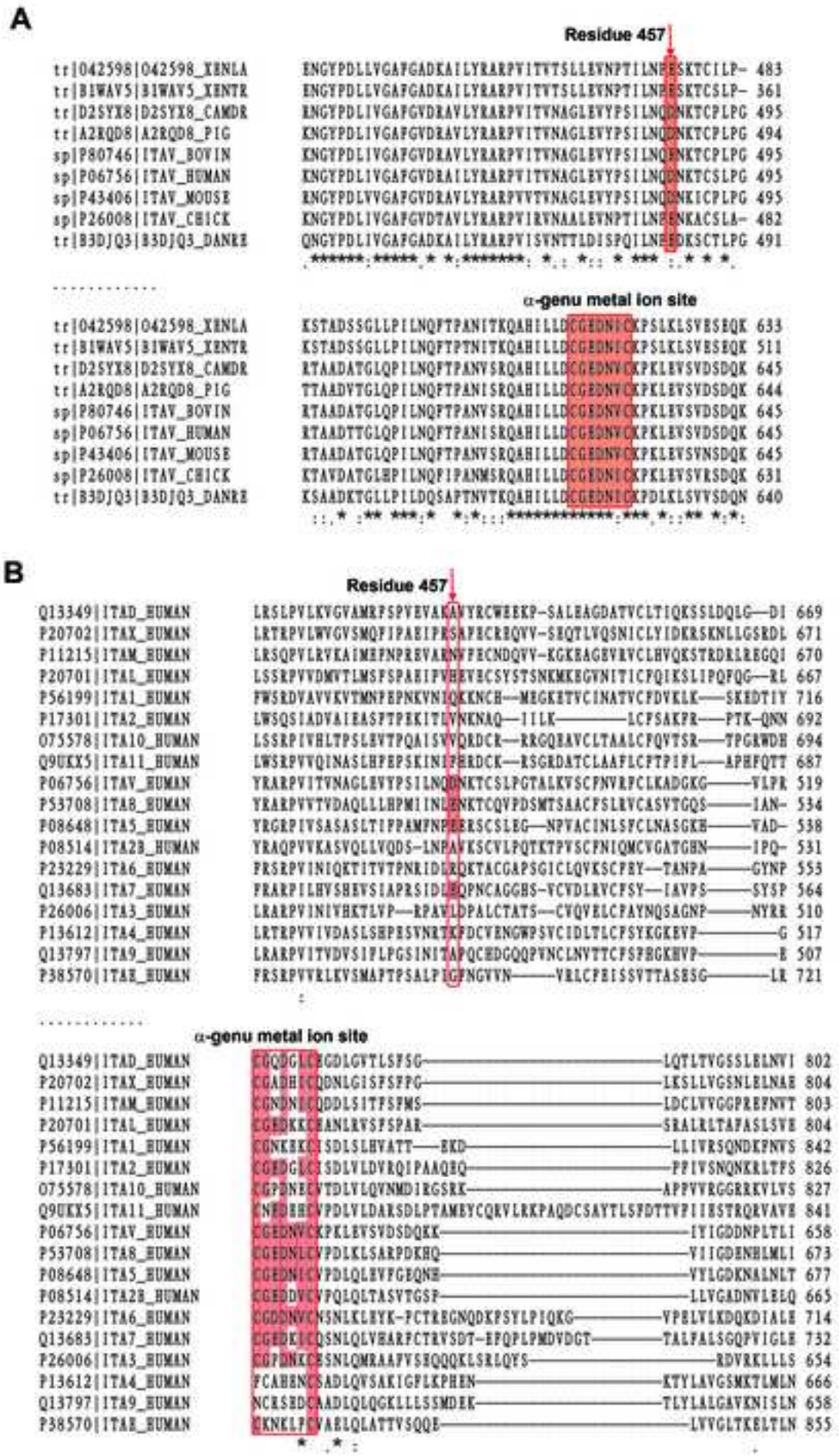

Supplemental Movie 1

Click here to download Supplemental Movies and Spreadsheets: movie1.avi

Supplemental Movie 2

Click here to download Supplemental Movies and Spreadsheets: movie2.avi

Supplemental Movie 3

Click here to download Supplemental Movies and Spreadsheets: movie3.avi

Supplemental Movie 4

Click here to download Supplemental Movies and Spreadsheets: movie4.avi

Supplemental Movie 5

Click here to download Supplemental Movies and Spreadsheets: movie5.avi

Supplemental Movie 6

Click here to download Supplemental Movies and Spreadsheets: movie6.avi